Thin Solid Films 587 (2015) 43–46

Contents lists available at ScienceDirect

Thin Solid Films

journal homepage: www.elsevier.com/locate/tsf

Fabrication and characterization of gold nanocrown arrays on a gold film for a high-sensitivity surface plasmon resonance biosensor

Munsik Choi [a], Nak-hyeon Kim [a], Seyoung Eom [a], Tae Woo Kim [b], Kyung Min Byun [a,*], Hyeong-Ho Park [c,*]

[a] Department of Biomedical Engineering, Kyung Hee University, Yongin 446-701, South Korea
[b] School of East–West Medical Science, Kyung Hee University, Yongin 446-701, South Korea
[c] Nano Process Division, Korea Advanced Nano Fab Center, Suwon 443-270, South Korea

ARTICLE INFO

Available online 20 November 2014

Keywords:
Surface plasmon
Nanocrown array
Nanoimprint lithography
Tilted evaporation
Sensitivity improvement

ABSTRACT

We report on a versatile method to fabricate gold nanocrown arrays on a thin gold film based on ultraviolet nanoimprint lithography and tilted evaporation technique. We realize highly ordered 2-dimensional nanocrown arrays and characterize their sizes and morphologies using scanning electron microscopy. To demonstrate an enhanced surface plasmon resonance (SPR) detection by the fabricated gold nanocrown samples, biosensing experiments are performed by measuring SPR angle shift for biotin–streptavidin interaction and bulk refractive index change of dielectric medium. We hope that the suggested plasmonic platform with a high sensitivity could be extended to a variety of biomolecular binding reactions.

1. Introduction

Surface plasmon (SP) is an electron density wave propagating along the metal–dielectric interface. Surface plasmon resonance (SPR) occurs under momentum matching between SP wave and incident light of transverse magnetic (TM) polarization. As this SPR condition is dependent on a refractive index of dielectric medium, change in resonance angle or wavelength can reflect the amount of adsorbed target molecules at the interface. By monitoring a shift of resonance signal, we can quantify the binding reactions of interest in a label-free way [1].

In recent years, metallic nanostructures have been employed in a conventional SPR system to improve a sensor sensitivity [2–4]. Contrary to propagating surface plasmons excited at a thin metal film, localized surface plasmons, the oscillation of free electrons confined to a finite nanoscale volume, can lead to a substantial confinement and enhancement of local electromagnetic fields [5,6]. In our previous study, we demonstrated that a local field enhancement is highly correlated with a sensitivity enhancement of SPR biosensor due to an intensified field–matter interaction [7]. Localized surface plasmons by metallic nanostructures may play a key role in realizing an ultrasensitive biomolecular detection.

Despite such important advantage, chemically synthesized nanoparticles may suffer from irregular positioning and thus it is still a major challenge to acquire designable and predictable properties from the bottom-up processes [8]. Also, to develop a desirable nanofabrication technique for substrate-bound nanostructures, several conspicuous features, including low-cost fabrication, large-area patterning, and reproducibility are essential. For this reason, alternative approaches such as nanosphere lithography, nanoimprint lithography (NIL), and stencil lithography appear to be preferable to conventional approaches, like electron-beam lithography and focused ion beam lithography [9]. While those conventional methods can provide a high resolution and a versatility [10], they are time-consuming and high-cost and also have a serious constraint on large-area production.

In this study, we introduce a fabrication process based on NIL and tilted evaporation technique to realize gold nanocrown arrays on a gold film. Nanoimprint is a stamp-based and mechanical lithographic method that can produce a large-area nanopattern with sub-10 nm resolution. Among several NIL approaches, we choose an ultraviolet (UV)-NIL because it is available in room temperature and is free from misalignment caused by different thermal expansion coefficients of the template and substrate. Also, tilted evaporation of titanium and gold is utilized to produce a complicated profile of gold nanocrown. After characterizing 2-dimensional nanocrown arrays by the use of field emission scanning electron microscope (FE-SEM), we test the sensing capabilities of the gold nanocrown samples by measuring a resonance angle shift when streptavidin binds to biotin and a bulk refractive index changes in an aqueous solution. Finally, by comparing the obtained results with the case of a conventional thin-film-based SPR structure, we intend to verify that gold nanocrown arrays are useful for improving the sensitivity performance significantly.

* Corresponding authors.
E-mail addresses: kmbyun@khu.ac.kr (K.M. Byun), hyeongho.park@kanc.re.kr (H.-H. Park).

http://dx.doi.org/10.1016/j.tsf.2014.11.047
0040-6090/

2. Experimental details

2.1. Fabrication of a thin gold film

An NSF10 glass with a square shape of 20×20 mm^2 was used as substrate. This substrate was cleaned in a hot piranha solution (7:3 mixture of H_2SO_4 and H_2O_2) for 1 min and rinsed with deionized water for 15 min and then dried with nitrogen gas. After a 5-nm thick titanium film for a strong adhesion between glass substrate and a gold film was applied onto an NSF10 glass substrate at a rate of 2 Å/s via electron-beam evaporator (UEE, Ultech), a 45-nm thick gold film was deposited in the same evaporation chamber. The fabricated sample was used as a control in biosensing experiments.

2.2. Fabrication of gold nanocrown arrays

To fabricate a working sample with gold nanocrown arrays on a gold film, serial processes of NIL, tilted evaporation, plasma etching and lift-off were performed. A polymethyl methacrylate (PMMA) layer was spin-coated on a gold film at 1000 rpm for 120 s and annealed at 170 °C for 5 min using a hot plate. For UV-NIL, 200 nm-thick UV-curable resin (NIP-SC28LV400, ChemOptics) was spin-coated on the 350 nm-thick PMMA layer at 2000 rpm for 60 s.

The silicon master containing hexagonal arrays was fabricated by deep ultraviolet lithography and deep reactive ion etching (RIE). The array holes of silicon master have a depth of 230 nm, a diameter of 300 nm and a period of 530 nm. Patterned polyurethane acrylate (PUA) mold is replicated from the silicon master by UV imprinting to acquire a flexible polymer mold [11,12]. Before imprinting, trichlorosilane (97%, Sigma-Aldrich) was applied on PUA mold for better separation between the mold and imprint resin [13]. The PUA mold was pressed using a nanoimprinter (NIL-8 imprinter, Obducat) at 2 MPa for 3 min. The UV-curable resin layer was then exposed to UV light for 2 min to induce a photochemical reaction and imprinted hexagonal hole arrays were formed on the resin.

After imprinting, residues on the resin layer were removed by a plasma asher (ALA-0601E, AMS). The imprinted patterns were transferred into PMMA layer by O_2 RIE (Versaline, Plasma-Therm). Following a deposition of 10-nm thick titanium adhesion layer, gold nanocrown array was produced by depositing a 50-nm thick gold layer using tilted evaporation technique. In this process, Au pellets are located at the edge within a chamber of electron beam evaporator and the sample is attached away from the center of rotation plate. While the plate is rotating, gold is deposited uniformly on the sample when the sample stands in line with the source. On the other hand, as the sample moves away from the source, slanted deposition may lead to an indented shape around the edges of hexagonal holes. A variety of morphologies in gold nanocrown can be obtained by controlling the speed of rotation and location of Au pellets. Finally, remaining PMMA and resin layers were removed by a lift-off process in an acetone solution under sonication. The obtained samples were characterized using FE-SEM (Leo Supra 55, Genesis 2000, Carl Zeiss) analyzer at 10 kV.

2.3. Biotin–streptavidin experiments

The fabricated samples were immersed in 1 mM 2-aminoethanethiol in ethanol for 10 h, followed by washing with ethanol and deionized water for 10 min. 340 μM NHS-PEG4-biotin (PN 21329, Thermo Scientific) in a phosphate buffered saline (PBS) solution (pH 7.4) was injected through the fluidic channel at a flow rate of 20 μL/min for 60 min using a peristaltic pump. After the immobilization of the biotin on the sample's surface, 400 nM streptavidin (PN 21122, Thermo Scientific) was injected into the fluidic channel at a rate of 20 μL/min for 60 min. After the binding reactions, the PBS solution was injected through the fluidic channel to wash the sensor chip and remove the unbound components. SPR signals were measured by an angle interrogation setup based on the Kretschmann configuration before and after the binding reactions.

3. Results and discussion

Fig. 1 illustrates the procedure to fabricate gold nanocrown arrays on a gold film. A 45-nm thick gold film is evaporated onto an NSF10 glass substrate after an evaporation of a 5-nm thick titanium adhesion layer. PMMA and UV-curable resin layers are then spin-coated before pressing the PUA mold. During the UV-NIL process, large-area patterns with a high feature density are transferred to the resin layer and subsequent UV exposure makes the imprinted pattern solid and stable. After the RIE process for deep etching of hole arrays, gold nanocrown array is formed by a tilted evaporation of titanium and gold. It should be noted that tilted evaporation induces a non-uniform deposition, especially in the sidewalls, resulting in a small peak at the center and an indented shape in round edges. Finally, the lift-off process is utilized to remove the residual components of PMMA and resin layers. As a result, a large-area gold nanocrown array on a gold film could be achieved in a reproducible way.

Fig. 2 shows the top-view and side-view FE-SEM images of the fabricated nanocrown samples. The average diameter, height, and pitch of gold nanocrown arrays are 380, 50, and 520 nm, respectively. Note that, a fairly increased diameter size of gold nanocrown, compared to 300-nm diameter of PUA mold, appears to be associated with the fact that severe dry etching processes can lead to a widening of nanohole array patterns. The coefficient of variation for the size is less than 5%, implying that the nanocrown arrays are realized with a good uniformity. The total effective area where nanocrown patterns are formed is approximately 15×15 mm^2.

Subsequently, in order to demonstrate the biosensing capabilities of the fabricated samples, SPR responses of gold nanocrown arrays on a gold film to biotin and streptavidin interaction and to change in the bulk refractive index were measured. While both sensitivity characteristics are frequently considered in estimating the sensor performance, the sensitivity obtained from layered interactions such as biotin–streptavidin interaction and DNA hybridization could be a more practical performance measure for an actual application [14].

We used custom-made Kretschmann-configuration optical setup to measure SPR signals. It was based on dual concentric motorized rotation stages (URS75PP, Newport, Irvine, CA) for angle scanning measurement with a nominal angular resolution at 0.002°. The setup employs a TM-polarized 10 mW He–Ne laser ($\lambda = 633$ nm, 25-LHP-991, CVI Melles Griot, Carlsbad, CA) as a light source and a calibrated photodiode (818-UV, Newport, Irvine, CA) as a photodetector. The fabricated SPR chips were index-matched to an SF10 prism. Two PDMS microfluidic channels (working and reference channels) were placed on top of the chip and screw-clamped to seal the channels.

Due to the angle scanning, the setup does not measure an interaction in real time. This is not a serious concern as far as this study is concerned, since we are interested only in the net resonance shift before and after an interaction, not details of intermediate kinetics. For the experiments of biotin–streptavidin interaction and bulk refractive index change, SPR curves were measured with a resolution of 0.01°. While the results are not shown here, the minimum value of measurable refractive index change was estimated to be 1×10^{-6} in refractive index unit (RIU) without any enhancement. The resonance angle was determined by fitting the reflectance curve to a second-order polynomial equation. Before SPR measurement, the reflectance characteristics of transverse electric polarization were recorded to eliminate common-mode noise components arising from the light source.

Fig. 3 shows SPR reflectance curves of conventional and nanocrown-mediated SPR samples. The solid black and red lines indicate the curves before and after an adsorption of streptavidin onto the biotin-functionalized substrate in a PBS environment. In Fig. 3(A), for a conventional SPR sample, the resonance angle shifts from 58.45° to

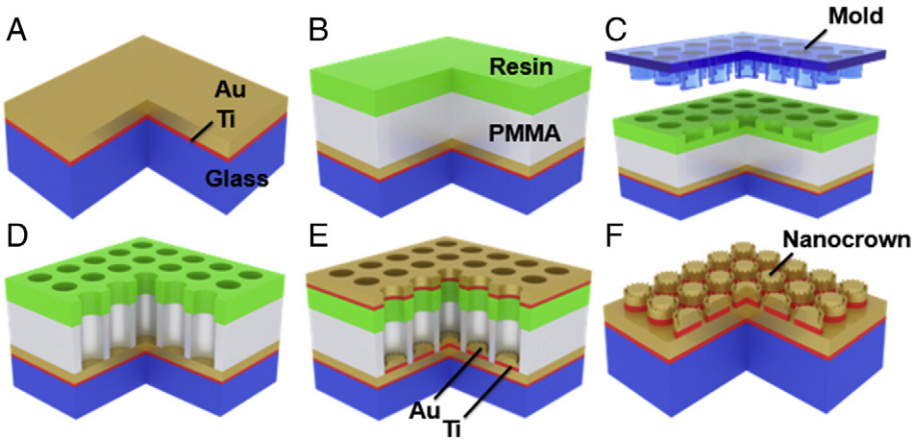

Fig. 1. Fabrication procedure of gold nanocrown arrays using UV-NIL and tilted evaporation. (A) Evaporating titanium and gold on a glass substrate, (B) spin-coating PMMA and imprint resin, (C) imprinting gold nanocrown array patterns, (D) etching imprint resin and PMMA, (E) depositing titanium and gold by tilted evaporation technique, and (F) lifting off the resin and PMMA.

58.67°; thus, the net change is 0.22°. By contrast, in Fig. 3(B), the resonance angles before and after injecting streptavidin are 60.46° and 60.79° for the sample with gold nanocrown arrays; thus, the resonance shift is 0.33°. As a quantitative measure of the sensitivity improvement, we suggest a sensitivity enhancement factor (SEF) that represents the impact of gold nanocrown on the detection sensitivity in reference to a conventional SPR biosensor. When SEF is defined as the ratio of resonance angle shift by a gold nanocrown-based SPR sample to that of a control one without any gold nanostructure, the results indicate that the introduction of gold nanocrown array to a gold film can offer an SEF = 150%.

The fabricated samples were then used to measure a bulk sensitivity when ethanol–water mixture was employed as dielectric media. Refractive indices of ethanol–water mixtures were measured by an Abbe refractometer (DR-M2, Atago Co., Japan). The results for the SPR angle shift as a function of the bulk refractive index are shown in

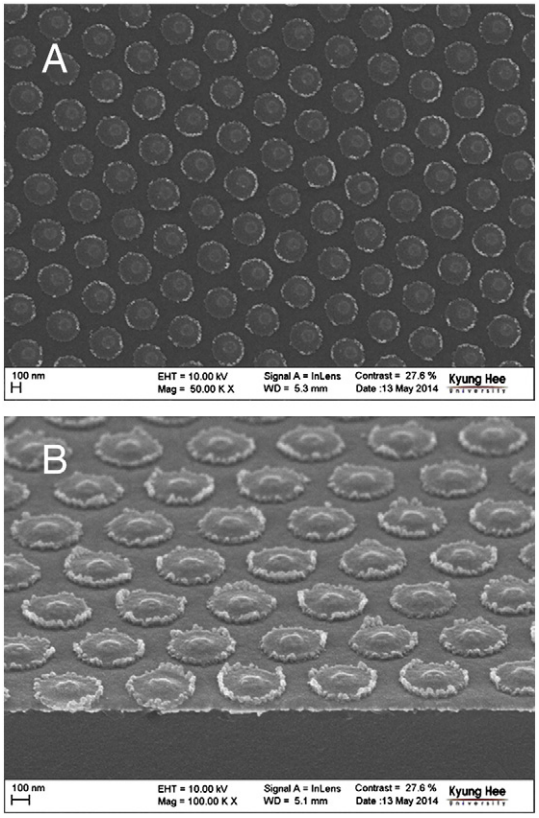

Fig. 2. (A) Top-view and (B) side-view FE-SEM images of gold nanocrown arrays with a diameter of 380 nm, height of 50 nm, and pitch of 520 nm. The total pattern area has a size of 15 × 15 mm^2.

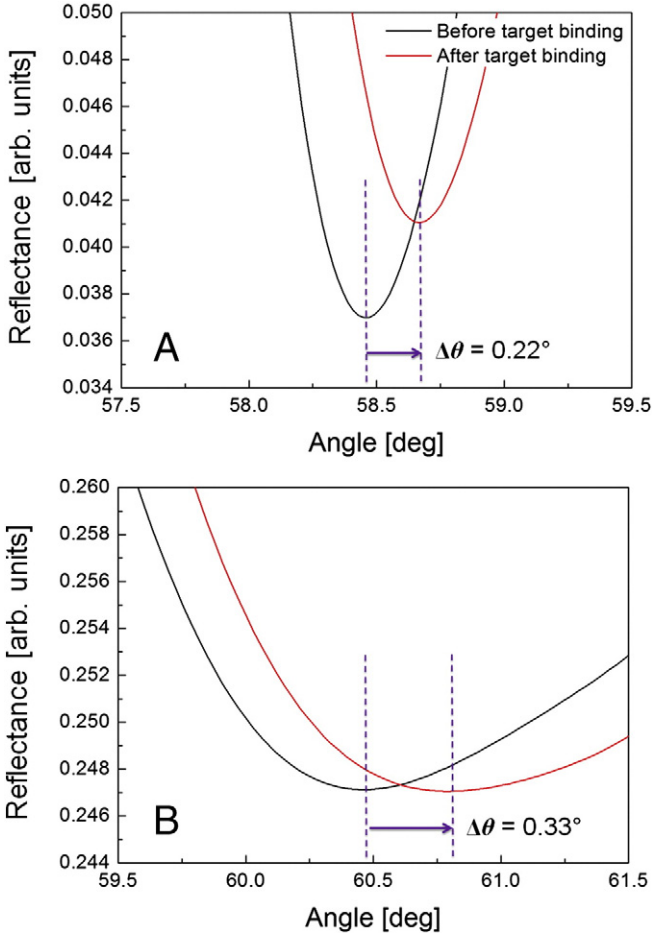

Fig. 3. SPR curves obtained from biotin–streptavidin interactions for (A) a thin gold substrate and (B) gold nanocrown arrays on a gold film. The black and red lines represent the results before and after injecting streptavidin biomolecules, respectively.

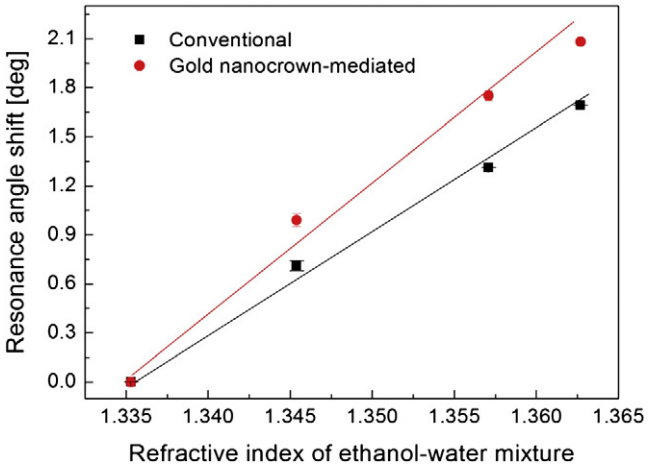

Fig. 4. Resonance angle shift according to a change in bulk refractive index of ethanol–water mixtures for the fabricated SPR samples with and without gold nanocrown arrays. The black and red lines indicate linear fits of experimental results.

Fig. 4 where the shift values are taken with respect to the result in pure water with $n = 1.335$ at $\lambda = 633$ nm. Resonance angle shift is fairly proportional to a refractive index of the media and more importantly, the bulk sensitivity is found to be higher for SPR substrate with gold nanocrown arrays. The obtained bulk sensitivities are 75.0°/RIU for gold nanocrown-mediated SPR sample and 60.2°/RIU for conventional one, implying that SEF is equal to 125%. This enhancement is not as high as the result in biotin–streptavidin experiments because SPR detection is intrinsically sensitive to a surface-limited change in refractive index. However, the bulk sensitivity experiment still supports that the proposed SPR system can be applicable even to the detection of concentration change of gases or liquids.

For both surface-limited changes by binding layer formation and increasing solution concentration in the above experiments, an interaction between local plasmon field and refractive index change within penetration depth plays a key role in producing a high sensitivity in plasmonic detection. Since gold nanocrowns are effective for a substantial enhancement of local electromagnetic fields at a finite nanoscale volume around their indented rim, they can produce an improved sensitivity through enhanced field–matter interaction. Based on such physical mechanism, field–matter interaction occurs more efficiently by the excitation of localized plasmons in the presence of gold nanocrown arrays, thereby resulting in an enhancement of detection sensitivity. In particular, guided ligand immobilization will allow target analytes with a low concentration to be bound onto the region with a high field intensity and therefore to produce an appreciable resonance shift. Moreover, it is anticipated that the detection sensitivity could be improved significantly via an additional optimization of the geometry or morphology of gold nanocrown arrays.

4. Conclusion

We have demonstrated the fabrication of a large-area gold nanocrown array on a gold film and the application for biomolecular detection. Highly ordered nanocrown arrays were realized reproducibly using UV-NIL and tilted evaporation technique that could allow a high-throughput fabrication of a sensitive plasmonic sensor platform. Surface-limited biosensing measurements and bulk sensitivity experiments confirmed that the proposed gold nanocrowns are useful for a high-sensitivity sensing applications. While a better understanding of the plasmonic behavior and the sensing response still requires further analysis, it should be noted that the use of gold nanocrowns can improve the sensitivity performance of a conventional SPR system significantly. We believe that the current study is an important step for implementing a plasmonic platform for a high sensitivity detection of biomolecular reactions.

Acknowledgments

We acknowledge the support of Korea Science and Engineering Foundation (KOSEF) grant funded by the Korean government (MEST) (NSF-2013R1A1A1A05011990 and 2013R1A2A2A04016066).

References

[1] J. Homola, S.S. Yee, G. Gauglitz, Surface plasmon resonance sensors: review, Sensors Actuators B 54 (1999) 3.
[2] L.A. Lyon, D.J. Pena, M.J. Natan, Surface plasmon resonance of Au colloid-modified Au films: particle size dependence, J. Phys. Chem. B 103 (1999) 5826.
[3] K.M. Byun, S.J. Yoon, D. Kim, S.J. Kim, Experimental study of sensitivity enhancement in surface plasmon resonance biosensors by use of periodic metallic nanowires, Opt. Lett. 32 (2007) 1902.
[4] L. Malic, B. Cui, T. Veres, M. Tabrizian, Enhanced surface plasmon resonance imaging detection of DNA hybridization on periodic gold nanoposts, Opt. Lett. 32 (2007) 3092.
[5] J.N. Anker, W.P. Hall, O. Lyandres, N.C. Shah, J. Zhao, R.P. Van Duyne, Biosensing with plasmonic nanosensors, Nat. Mater. 7 (2008) 442.
[6] A.J. Haes, S. Zou, G.C. Schatz, R.P. Van Duyne, Nano-scale optical biosensor: short range distance dependence of the localized surface plasmon resonance of noble metal nanoparticles, J. Phys. Chem. B 108 (2004) 6961.
[7] N.H. Kim, W.K. Jung, K.M. Byun, Correlation analysis between plasmon field distribution and sensitivity enhancement in reflection- and transmission-type localized surface plasmon resonance biosensors, Appl. Opt. 50 (2011) 4982.
[8] T. Sannomiya, C. Hafner, J. Voros, In situ sensing of single binding events by localized surface plasmon resonance, Nano Lett. 8 (2008) 3450.
[9] S.W. Lee, K.S. Lee, J.H. Ahn, J.J. Lee, M.G. Kim, Y.B. Shin, Highly sensitive biosensing using arrays of plasmonic Au nanodisks realized by nanoimprint lithography, ACS Nano 5 (2011) 897.
[10] A. Perentes, I. Utke, B. Dwir, M. Leutenegger, T. Lasser, P. Hoffmann, F. Baida, M.P. Bernal, M. Russey, J. Salvi, D.V. Labeke, Fabrication of arrays of sub-wavelength nano-apertures in an optically thick gold layer on glass slides for optical studies, Nanotechnology 16 (2005) 273.
[11] S.J. Choi, P.J. Yoo, S.J. Baek, T.W. Kim, H.H. Lee, An ultraviolet-curable mold for sub-100-nm lithography, J. Am. Chem. Soc. 126 (2004) 7744.
[12] K.Y. Suh, H.E. Jeong, D.-H. Kim, R.A. Singh, E.-S. Yoon, Capillarity-assisted fabrication of nanostructures using a less permeable mold for nanotribological applications, J. Appl. Phys. 100 (2006) 034303.
[13] J.Y. Kim, D.-G. Choi, J.-H. Jeong, E.-S. Lee, UV-curable nanoimprint resin with enhanced anti-sticking property, Appl. Surf. Sci. 254 (2008) 4793.
[14] O. Vazquez-Mena, T. Sannomiya, L.G. Villanueva, J. Voros, J. Brugger, Metallic nanodot arrays by stencil lithography for plasmonic biosensing applications, ACS Nano 5 (2011) 844.